International Journal of
Mathematical Modelling & Computations
Vol. 13, No. 03, Summer 2023, 1- 13
DOI:10.30495/ijm2c.2023.1991902.1279

Presenting a Novel Sensitivity-Damage Feature for Damage Detection Using Time-Series Analysis, Output-Only Ambient Vibration Data

S. A. Hashemi[a], B. Adhami[a,*] and A. Golsoorat. Pahlaviani

[a]*Department of Civil Engineering, Central Tehran Branch, Islamic Azad University, Tehran, Iran.*

Abstract. This paper presents a damage identification method for a benchmark structure model using time series analysis of output-only ambient vibration data. To demonstrate the capability of the proposed method, a 3D finite element model based on a benchmark laboratory model is simulated, and a novel damage-sensitivity feature based on autoregressive time series models with exogenous input (ARX) using the output acceleration responses from the sensors. , is presented under the influence of ambient loads in modeling. In the finite element model, minor local damages near the supports that may occur to a bridge during operation are created to demonstrate the robustness and stability of the proposed damage feature. The results showed that the presented damage feature could effectively identify and locate the minor damages made near the supports (which is presented as a challenge in identification studies) accurately and without errors and provide an indication of the extent of the damage.

Received: 07 July 2023, Revised: 28 August 2023, Accepted: 18 September 2023.

Keywords: Damage identification, Benchmark structure, Damage-sensitivity feature, Ambient loads.

Index to information contained in this paper

1. Introduction

In recent years, Structural Health Monitoring (SHM) has received significant attention in aerospace, mechanical, and civil engineering. The SHM refers to the monitoring and investigating of changes in structures over a specific time to detect, locate, and determine the level of damage and assess the possibility of continued use of the structure and estimate its lifetime. Various definitions of damage can be proposed. For example, damage is defined as changes introduced to the system that have an undesirable effect on the current and future performance of the system [4]. There are various methods for implementing SHM, among which visual inspection is the most important. Although this method is considered a qualitative approach because it can be carried out periodically, quantitative methods include global and local measurements. For example, non-destructive evaluation techniques, which are mostly local, can provide more accurate and detailed information on damage, but these methods are also periodic, like a visual inspection. To overcome this drawback, permanent monitoring systems that include a network of sensors and evaluate the overall behavior of the structure can be used [12]. One of the important subsets of vibration-based methods is time series methods. Time series is a part of general methods

[*]Corresponding author. Email: beh.adhami@iauctb.ac.ir

https://sanad.iau.ir/journal/ijm

that are the most accurate and efficient methods for detecting and evaluating the damage. This method has advantages such as no requirement for visual inspection, automation capability, coverage of the entire structure, no requirement for finite element models, etc. [5,6,7,15]. Numerous studies have been conducted to identify damage based on time series to extract damage-sensitive features (DSF). For example, Sohn and Farrar used a method based on a time series analysis of vibration signals to detect and locate damage in a mechanical system. They utilized the standard deviation of residual errors, which is the difference between measured and predicted acceleration, extracted from hybrid AR[1]-ARX[2] models as damage-sensitivity features [19]. Lu and Gao introduced the ratio of the standard deviation of residual error in the actual (damaged) system to that in the initial (undamaged) state as a damage-sensitivity feature and used the ARX model for prediction signals. They also investigated that although the deviation of residual error of the ARX model is sensitive to damage, it does not provide an accurate index of the damage level [13]. Nair et al. introduced a function of the first three components of AR as damage features and used the ARMA[3] model for time series modeling. They used a hypothesis t-test for damage detection and introduced two indices based on AR coefficients for damage localization. They tested their proposed method on analytical and experimental results of ASCE benchmark structures [17].

Catbas and Gul presented a statistical pattern recognition methodology using various laboratory structures. They used the AR model with the Mahalanobis distance-based outlier detection algorithm for damage identification and evaluated their method using two different laboratory structures. They utilized AR coefficients as a damage feature. Their results showed that successful identification was achieved in both laboratory models, although their method failed in some cases for one of the laboratory models [9]. In addition, Catbas and Gul presented a new method based on time series analysis using ARX models with different clusters and using the free response of the structure to detect, locate, and estimate the extent of the damage. They proposed two different approaches for introducing damage features from ARX models for different clusters. The first approach was introduced based on the direct comparison of coefficients of ARX models. In this approach, identification is not successful if there is noise in the system. Therefore, where the system is noisy and when the model becomes more complex, the second approach was introduced as a damage feature. This approach is based on fitting ratios from ARX models [10]. In another study, Catbas and Gul presented a time series analysis method for detecting damage using output-only vibration data and used ARX models to simulate this data. They introduced the difference between fit ratios as a damage feature. This method was applied to experimental data from a steel grid structure with different damage scenarios. Ambient vibration tests showed that damage could be successfully identified and located using this method. In addition, the relative level of damage was estimated using this method. However, this method does not work accurately in cases where the damage is small. The aforementioned damage detection method was applied to the Z24 bridge, and the results showed that this method could identify the location and severity of damage satisfactorily [8].

In several studies, Mita et al. proposed a substructure approach using time series to detect local damage in a shear structure. They used a hybrid damage feature based on both the model coefficients and residuals of the ARMAX[4] model and showed that complete information about the structural damage could be obtained compared to the case where only model coefficients are used in the damage feature [14,23,24]. Farahani and Penumadu

---

[1] Autoregressive (AR)
[2] Autoregressive with Exogenous Input (ARX)
[3] Autoregressive Moving Average (ARMA)
[4] Autoregressive Moving Average with Exogenous Input (ARMAX)

presented a parametric study to understand the effects of damage location, extent, and vibration measurement noise using time series-based damage identification techniques. They used a new damage-sensitive feature based on prediction errors of the ARX model and found that the damage location cannot be identified when the damage is near support on an internal main girder [21]. Azim and Gul proposed a method for identifying damage in railway bridges based on acceleration responses. They used ARX models in the introduced damage feature and introduced the differences between fitting ratios as the damage feature. Their results showed good agreement between the predicted and expected damage features. One of the limitations of the aforementioned method is that although small local damages can be detected, their precise location is difficult to determine [2]. Catbas et al. investigated the ability of the ARX model analysis method to detect damages/flaws in Composite Overwrapped Pressure Vessels (COPVs) using pressure as input and corresponding strains as response data. They introduced a damage feature based on the difference in fitting ratios between healthy and damaged states for comparing the existing conditions of COPVs [16]. Chegeni et al. also introduced an effective one-variable similarity method called Kolback similarity (KS) for locating the damage and identifying the severity of the damage. They used a feature extraction technique based on residual to determine a sufficient order of the AR model that can extract independent residual [11].

The study presented a damage identification method based on time series analysis for a benchmark laboratory structure. In this regard, a finite element model was used to simulate the laboratory model used in previous studies [8,9,10]. The main goal of this study is to provide a new method for effective damage identification, localization, and estimation of damage severity. As observed, a powerful method has not been proposed for detecting damage around supports, especially when damages are small and local. Therefore, in this study, to compensate for this weakness, a new damage feature was introduced to correctly identify such damages, which in previous studies mostly suffered from false positive and negative results. The following will be discussed in this section, including the fundamentals of methodology such as time series modeling and governing equations, system identification structure, damage-sensitivity feature extraction, threshold determination, finite element modeling of the benchmark structure and introduction of various damage scenarios, modeling assumptions, inputs, outputs, and the application of the proposed method, discussion and analysis of results, and finally, conclusion.

2. Methodology fundamentals

2.1 *Time series modeling*

As shown in Figure 1, a linear time-invariant (LTI) system can be considered with a white noise input and a colored process output. By considering Equation (1) of time series models:

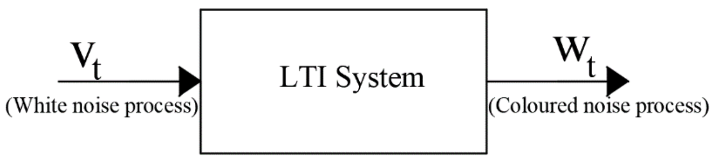

Figure 1. Modeling a colored random process

$$d_0w_t + d_1w_{t-1} + d_2w_{t-2} + \cdots + d_nw_{t-n} \\ = c_0v_t + c_1v_{t-1} + c_2v_{t-2} + \cdots + c_mv_{t-m} \quad (1)$$

Equation (1) expresses a relationship between white noise (input) and colored noise (output). The above model is known as an ARMA time series model. Now, if the coefficients c are equal to zero and the coefficient of $c_0 = 1$, the special case of the AR model is obtained. And if the coefficients d are equal to zero and the coefficient of $d_0 = 1$, the special case of the MA model is obtained. Usually, the values of $c_0 = 0$ and $d_0 = 1$ are assumed to be unique solutions. Now, assuming that the system transformation function is equal to $\frac{B(Z^{-1})}{A(Z^{-1})}$ and the x_t input is applied to the system, the output without noise and system errors can be represented by $\tilde{y}$ (which is not accessible), and the noise and errors present in the system can be shown together as w_t.

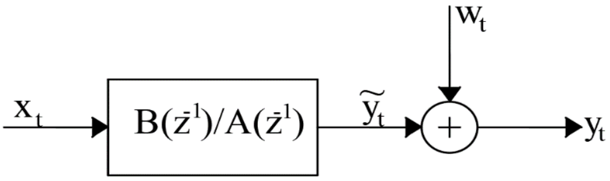

Figure 2. Structural and measurement errors in the form of colored noise applied to the system.

By combining Figures 1 and 2, the general structure of the ARMAX system can be obtained, as shown in Figure 3.

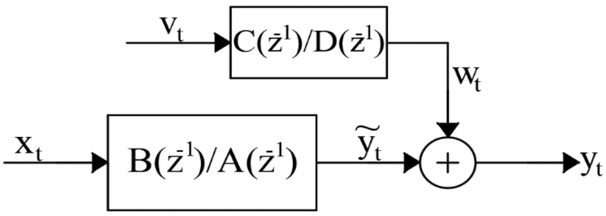

Figure 3. ARMAX block diagram according to relation (2).

This structure can be written in the form of relation (2):

$$y_t = \frac{B(z^{-1})}{A(z^{-1})}x_t + \frac{C(z^{-1})}{D(z^{-1})}v_t \quad (2)$$

But generally, for the simplicity of calculations, the ARMAX formula is considered as equation (3):

$$A(z^{-1})y_t = B(z^{-1})x_t + \underbrace{C(z^{-1})v_t}_{e_t} \quad (3)$$

In other words, a MA model is considered for e_t signal. Now if e_t is white noise, the resulting model is an ARX. Equation (4) represents the general form of the ARX time series.

$$y(t) + \sum_{k=1}^{n_a} a_k\, y[t-k] = \sum_{k=n_k}^{n_b} b_k\, x[t-k] + e_t \quad (4)$$

a_k‘ b_k are the unknown parameters of the model, n_a, n_b, n_k respectively are the order of AR, the order of input X and the order of delay, and e_t is the residual of the model.

2.2 *System identification structure*

This article uses a method for damage detection using output-only ambient vibration data by applying ARX time series models and sensor clustering [8,10], and the acceleration vibration data is recorded from each sensor. Before fitting time series models to sensor data, the data is normalized (standardization) according to equation (5) [17,19] to compare acceleration histories at a sensor location, which may have occurred under different environmental and operational conditions.

$$\hat{y}_i(t) = \frac{y_i(t) - \mu_i}{\sigma_i} \tag{5}$$

where $\hat{y}_i(t)$ is the normalized acceleration signal in sensor i and $y_i(t)$ is the acceleration signal in sensor i, μ_i, σ_i are respectively the mean and standard deviation of the acceleration in sensor i (in the following, $y(t)$ is used instead of $\hat{y}(t)$ for convenience). Obtaining the free response of the structure for most civil engineering applications may not be an easy task. In this article, the random decrement (RD) technique is used to obtain the quasi-free response data from the ambient vibration data similar to that found in the references [8,9,20]. The random decrement method was first developed by Cole (1968) and is used to transform random time series into a free decreasing response. The RD method can eliminate the effects of random loading on the structure and makes it easier to fit time series models to the data. After the normalization (standardization) of acceleration data, the RD method was used to obtain quasi-free response data. Then several sensor clusters are created for adjacent sensors, and for each cluster, multi - input – single-output ARX time series models are generated for the structure in healthy conditions. According to equation (6) and Figure 4, which shows an ARX model, for each of the clusters, the input of the model (x(t)) acceleration responses, including all the degrees of freedom of that cluster and the output of the ARX y(t)) model is the acceleration response of the reference channel.

$$A(z^{-1})y(t) = B(z^{-1})x(t) + e(t) \tag{6}$$

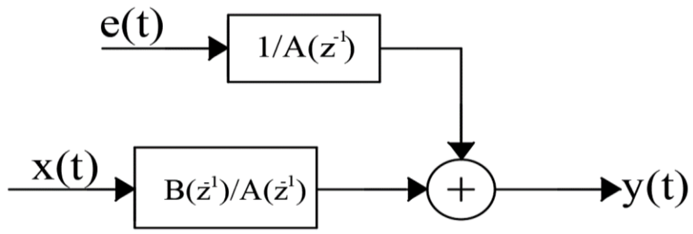

Figure 4. ARX block diagram according to relation (6).

After the ARX models in healthy conditions are produced for each cluster, the same models are used to predict the vibration data obtained in damaged conditions in the same cluster.

2.3 *Extracting damage sensitivity features*

The definition of a damage feature that is sensitive to changes in the system is one of the most important steps in the effective identification of the system. The damage feature is defined based on the coefficients and residuals of the model. Many studies have been conducted in this regard, mostly based on either model coefficients or model residuals, leading to false positive or negative results in the identification process. More accurate information about the system can be obtained by defining a damage feature that can encompass both parts. Therefore, in this study, a new hybrid damage feature, which includes both model coefficients and residuals, is introduced according to equation (7).

$$\mathrm{DSF} = \frac{\sigma(\mathrm{e_d})}{\sigma(\mathrm{e_h})} \cdot \frac{\left||\bar{c}_{3h}| - |\bar{c}_{3d}|\right|}{|\bar{c}_{3h}|} \cdot \frac{\omega_h}{\omega_d} \tag{7}$$

As it is known, the equation consists of three parts .In the first part of equation (7), parameter ($\frac{\sigma(e_d)}{\sigma(e_h)}$) is the ratio of the standard deviation of the residual error in the damaged state to the standard deviation of the residual error in the healthy state. In the definition of e_h and e_d, the responses of y_h, y_d, and $\hat{y}$ according to equation (8), are equal to the acceleration response in the healthy state, the acceleration response in the damaged state, and the predicted response, respectively. Many studies have been carried out based on the first part of relation (7) as a feature of damage. And in their investigations, it was found that this relationship does not provide an accurate indicator of the damage level, and sometimes they get false results in locating the damage.

$$e_h = y_h - \hat{y} \qquad\qquad e_d = y_d - \hat{y} \tag{8}$$

The definition of the second part of the equation (7), that is ($\frac{\left||\bar{c}_{3h}|-|\bar{c}_{3d}|\right|}{|\bar{c}_{3h}|}$), it shows the changes in the average of the first three coefficients of the AR model, where $\bar{c}_{3h}$ and $\bar{c}_{3d}$ are respectively the norm average of the first three coefficients of the AR model in a healthy and damaged state, in order to achieve The most effective result, the number and different states of the coefficients, were considered and it was determined that the first three coefficients with the aforementioned combination, in the second part of the equation (7), gives a damage feature, sensitive to changes in the system. The third part of equation (7) or ($\frac{\omega_h}{\omega_d}$) is the ratio of the original frequency in the healthy state to the damaged state in each cluster.

2.4 *Definition of threshold*

To distinguish for changes in the damage-sensitive features due to noise and changes resulting from damage, an approach is introduced to define the threshold value based on noisy data in healthy conditions similar to [10,22], where a Monte Carlo simulation was used. Additionally, a set of 10% white noise data is separately added, and this process is repeated independently 1000 times. With each iteration, the damage feature is calculated, and its features are sorted from lowest to highest. To achieve a 95% confidence level, the 950th feature value is selected as the threshold value. Finally, any value above this threshold is considered damage, and any value below the threshold, which may be due to the presence of damage or noise in the data, is not considered damage.

2.5 *Finite element model construction of the benchmark structure*

This article uses a benchmark structure for numerical study [3,8]. The structure mentioned above is a grid steel model representing the primary phase of the study on the practical behavior of bridges. A finite element model of the benchmark structure is constructed using ABAQUS [1] (Figure 5).

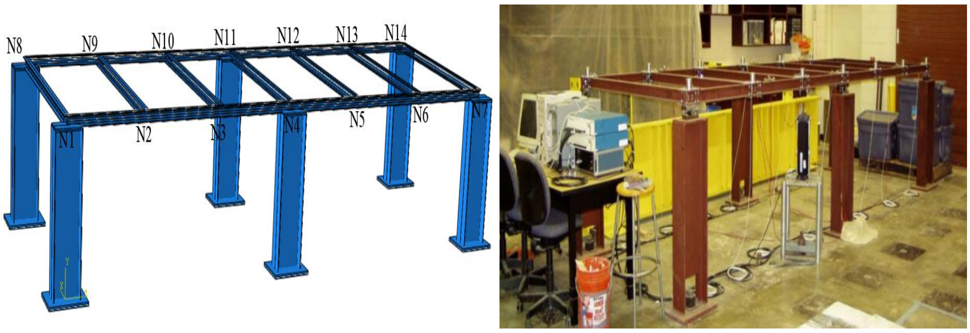

Figure 5. Laboratory physical model of the University of Central Florida benchmark structure - Catbas et al.- (right). Finite element benchmark structure model based on [3,8] (left).

The columns on the ground level were modeled as fixed supports. The superstructure is supported by four columns with roller connections (N4, N7, N11, N14) and two columns with hinge connections (N1, N8). The finite element model consists of 5145 nodes and 3744 members. Table 1 shows the material properties and selected steel sections. To validate the model used in this study for simulating the behavior of the bridge under healthy conditions, modal analysis was performed, and the natural frequencies and mode shapes obtained from the model were compared with the experimental data. Additionally, in Abaqus software, all elements of the model were selected as standard shell elements - four-node and two-curve reduced integration elements (S4R).

Table 1. Properties of materials and sections used in the finite element model [3,8].

Materials	**Poisson's ratio**	**Density (Ton/mm3)**	**Elastic modulus (MPa)**	**Column section**	**The cross-section of the girder**	**The cross-section of the cross beam**
Steel	0.3	7.85 e^{-9}	2 e^{5}	W10X26	S3X5.7	S3X5.7

In order to validate, the first four principal modes of the model under investigation were examined. In Figure 6, the shapes of the first four modes of the model and those identified experimentally by Catbas et al. in healthy structural conditions are shown. As can be observed, the modal shapes of the model exhibit good agreement with the modal shapes identified from experimental data. To quantify the amount of correlation between the modal shapes obtained from the models and those identified from experimental data, the Modal Assurance Criterion (MAC) [18] was used according to equation (9). The MAC is a value between zero (indicating not consistent mode shapes) and one (indicating fully consistent mode shapes). Values greater than 0.9 indicate (consistent correspondence) high compatibility, while small values indicate low (weak) similarity between the two modal shapes.

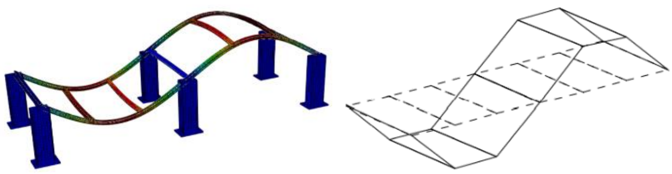

(a) The shape of the first mode.

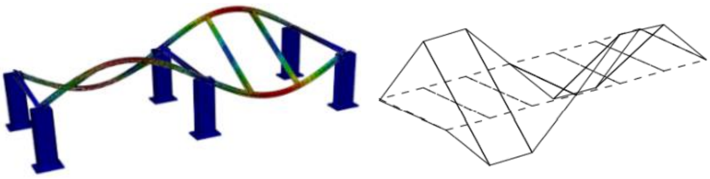

(b) The shape of the second mode.

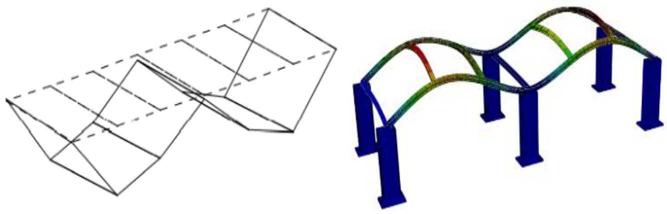

(c) Third mode figure.

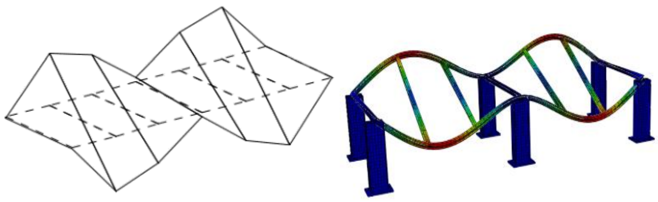

(d) Fourth mode figure.

Figure 6. Comparison of mode shapes in a healthy state: finite element model (right), laboratory model (left)

$$\mathrm{MAC(E, FE)} = \frac{\left|\sum_{j=1}^{n}\{\varphi_E\}_j\,\{\varphi_{FE}\}_j\right|}{\left(\sum_{j=1}^{n}\{\varphi_E\}_j^2\right)\left(\sum_{j=1}^{n}\{\varphi_{FE}\}_j^2\right)} \tag{9}$$

In equation (9), $\{\varphi_E\}$ is the experimental mode vector and $\{\varphi_{FE}\}$ is the mode vector resulting from the finite element model. As Table 2 shows the modal frequencies and MAC values for the first four principal modes, the maximum difference between the frequencies of the modes is equal to 5% and the MAC values are greater than 0.9, which indicates a good correlation between the mode shapes of the finite element and the laboratory model.

Table 2. Comparison of natural frequencies and mode shapes, finite element, and laboratory model.

Vertical mode	Limited components	Experimental	% error	MAC
Mode 1	22.13 Hz	22.37 Hz	-1.072	1
Mode 2	27.729 Hz	27Hz	2.7	1
Mode 3	31.709 Hz	33.38 Hz	-5	0.995
Mode 4	40.931 Hz	40.91 Hz	0.05	0.995

2.6 *Assumed damage scenarios*

In this study, a damage case with different levels has been considered according to Table 3. The damage case related to the settlement of the support under column 1 (under the column connected to node N1 according to Figure 7) is assumed as a damage scenario.

Table 3. Damage scenario.

Damage state	Description of damage mode
Settlement	D1. 40 millimeters settlement under column 1
	D2. 50 millimeters settlement under column 1
	D3. 70 millimeters settlement under column 1
	D4. 100 millimeters settlement under column 1

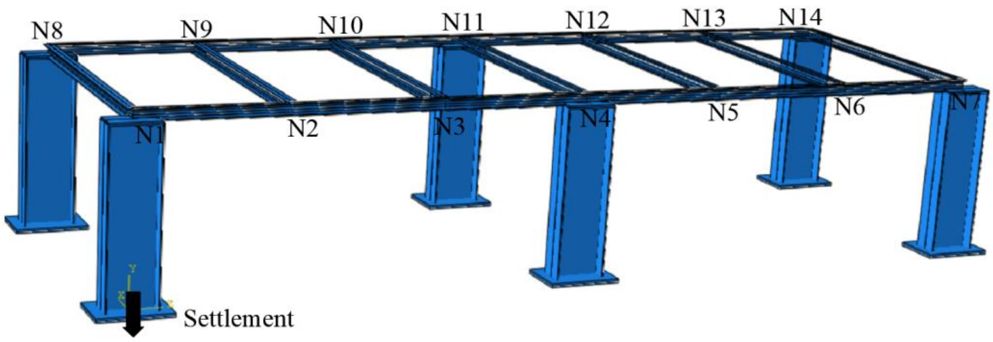

Figure 7. Assumed damage scenario.

2.7 *Assumptions for modeling, inputs, outputs, and implementation of the proposed method*

White Gaussian noise has been used to define ambient loads as an input to the structure. In the benchmark model of the bridge, according to Figure 5, accelerations were taken from eight nodes, except for the supports, to collect vertical accelerations (accelerations near zero are obtained at the supports, which may cause instability in modeling time series). The sampling interval is 0.01, and to consider the instrumental and measurement errors in the sensors, 10% of white Gaussian noise has been added to the acceleration responses. After collecting the ambient vibration data in healthy and damaged states, the data have been normalized (standardization) according to equation (5) to compare acceleration histories in a sensor location that may have occurred under different environmental and operational conditions. Then, the random decrement method was used to eliminate the effects of random loading on the structure, facilitate the fitting of time series models, and reach the quasi-free response data from the ambient vibration data. Several clusters are created for neighboring sensors, according to Table 4 and Figure 8. For each cluster, multi-input single-output (MISO) ARX time series models are generated in the healthy state. Suitable orders of models have been selected using the Akaike Information Criterion (AIC) and the Final Prediction Error (FPE). ARX time series models have also been generated in the damaged state (according to the introduced damage scenario in Table 3). The response in the damaged state is predicted using the healthy condition. Then, the damage-feature sensitivity is applied. The threshold value is obtained as explained, equal to 0.4226. This method is schematically and briefly illustrated in Figure 9.

Table 4. Input and output of ARX models generated and used for finite element modeling.

Sensor cluster	ARX model output (reference channel)	ARX Model Input
1	N2	N2,N9,N3
2	N3	N2,N3,N10,N5
3	N5	N3,N5,N12,N6
4	N6	N5,N6,N13
5	N9	N9,N2,N10
6	N10	N9,N10,N3,N12
7	N12	N10,N12,N5,N13
8	N13	N12,N13,N6

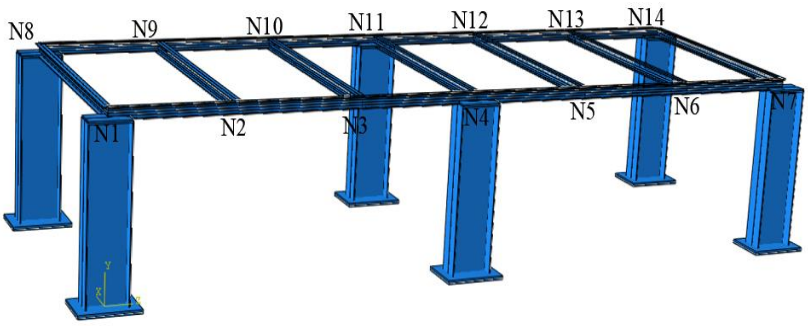

Figure 8. Sensor clustering for finite element model according to Table 4.

3. Discussion and analysis of results

3.1 *Settlement damage*

According to Figure 7, settlement under the column connected to N1 in four scenarios with values of 40, 50, 70, and 100 millimeters has been considered. The results are shown in Figure 10, where Cluster 1, which is the closest sensor location to the damage location, has the highest values of damage features and exceeds the threshold value. Therefore, Cluster 1 accurately represents the existence and location of the damage. With an increase in settlement values, the damage feature values also increase. Additionally, when the settlement value is equal to 100 millimeters, Cluster 2 (N3 in Figure 7) also has a value greater than the threshold value. This is because the sensor is located at position N3, which is the closest location to sensor N2 and is located on the same girder. Therefore, it is less affected by the settlement value and has fewer damage features than N2. In general, it can be concluded that in this case of damage, the damage feature accurately identifies the existence and location of the damage and are able to obtain a relative intensity index of the damage.

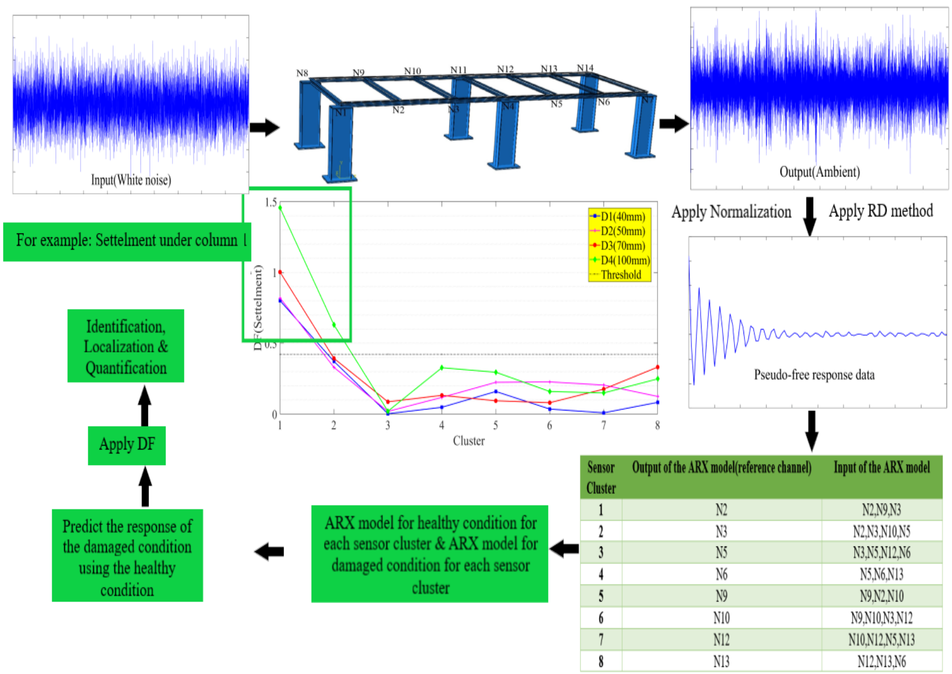

Figure 9. Graphical abstract.

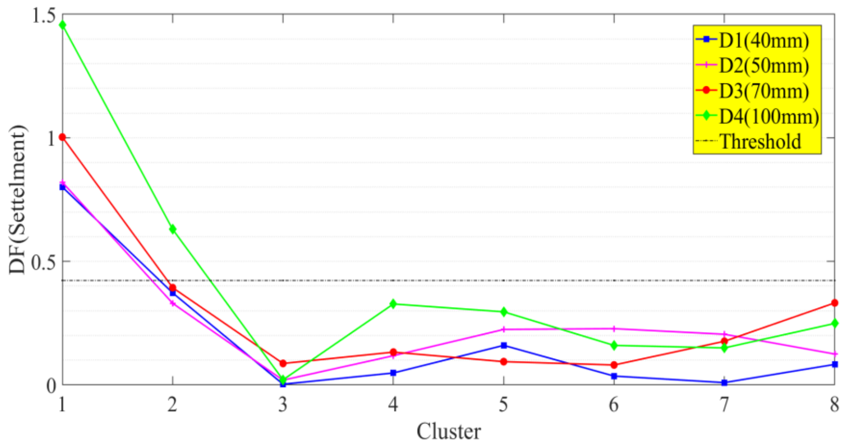

Figure 10. The damage feature obtained for the settlement of column 1 from ambient vibration data with a 10% noise level.

4. Conclusion

Using ARX time series models to identify hypothetical damage scenarios, a new damage feature has been introduced. The introduced damage feature uses a combination of model coefficients and model residuals for more accurate identification. Small and localized damage scenarios were investigated to demonstrate the superiority and capability of the proposed feature. The analysis results show that the introduced damage feature can effectively identify and locate assumed damages and estimate their extent. A notable advantage of this research is the defined scenario in which the damage is assumed to be near the support point of the assumed structure. This type of damage, which has been a significant challenge in most previous studies, has been effectively identified in terms of localization and extent estimation for various damage severity levels by the proposed damage feature. The study did not consider the effect of multiple and simultaneous damages and various, sometimes smaller, damage scenarios. Therefore, in future studies, authors will consider this issue.

References

[1] ABAQUS version 2017. Providence, RI, Dassault Systèmes Simulia Corp, (2016).

[2] M. R. Azim and M. Gul, Damage detection of steel girder railway bridges utilizing operational vibration response, Structural Control and Health Monitoring, **26** (2019) e2447.

[3] J. L. Burkett, Benchmark Studies for Structural Health Monitoring Using Analytical and Experimental Models, Electronic Theses and Dissertations, **436** (2005).

[4] R. Farrar and K. Worden, An introduction to structural health monitoring, Philosophical Transactions of the Society A, **365** (2007) 303–315.

[5] S. D. Fassois and F. P. Kopsaftopoulos, Statistical Time Series Methods for Vibration Based Structural Health Monitoring. In: W. Ostachowicz and J. Güemes (eds), New Trends in Structural Health Monitoring, CISM International Centre for Mechanical Sciences, Springer, Vienna, **452** (2013) 209–264, doi:10.1007/978-3-7091-1390-5_4.

[6] S. D. Fassois and J. S. Sakellariou, Statistical time-series methods for structural health monitoring, John Wiley & Sons Ltd, (2009) 443–472.

[7] S. D. Fassois and J. S. Sakellariou, Time series methods for fault detection and identification in vibrating structures, Philosophical Transactions of the Royal Society: Mathematical, Physical and Engineering Sciences, **365** (2007) 411–448.

[8] M. Gul and N. Catbas, Damage assessment with ambient vibration data using a novel time series analysis methodology, Journal of Structural Engineering, **137 (12)** (2011) 1518–1526.

[9] M. Gul and N. Catbas, Statistical pattern recognition for structural health monitoring using time series modeling: Theory and experimental verifications, Mechanical Systems and Signal Processing, **23 (7)** (2009) 2192–2204.

[10] M. Gul and N. Catbas, Structural health monitoring and damage assessment using a novel time series analysis methodology with sensor clustering, Journal of Sound and Vibration, **330** (2011) 1196–1210.

[11] M. Haghani Chegeni, M. K. Sharbatdar, R. Mahjoub and M. Raftari, A novel method for detecting structural damage based on data-driven and similarity-based techniques under environmental and operational changes, Numerical Methods in Civil Engineering, **6 (4)** (2022) 16–28.

[12] N. Johnson, Global and Local Structural Health Monitoring Methods Based on Wireless Telemetry and Boundary-based Thermography, University of Michigan, Ph.D. Dissertation, (2017).

[13] Y. Lu and F.Gao, A novel time-domain auto-regressive model for structural damage diagnosis, Journal of Sound and Vibration, **283** (2005) 1031–1049.

[14] L. Mei, A. Mita and J. Zhou, An improved substructural damage detection approach of shear structure based on ARMAX model residual, Structural Control and Health Monitoring, 23 (2016) 218–236.

[15] P. G. Michaelides, P. G. Apostolellis and S. D. Fassois, Vibration–based damage diagnosis in a laboratory cable–stayed bridge model via an RCP–ARX model based method, Journal of Physics Conference Series, Journal of Physics: Conference Series, **305** (2011) 012104.

[16] A. J. Modesto, R. Birgul, R. J. Werlink and F. N. Catbas, Damage detection of composite overwrapped pressure vessels using ARX models, International Journal of Pressure Vessels and Piping, **192** (2021) 104410.

[17] K. Nair, A. Kiremidjian and K. Law, Time series-based damage detection and localization algorithm with application to the ASCE benchmark structure, Journal of Sound and Vibration, **291** (2006) 349–368.

[18] M. Pastor and M. Binda and T. Harcarik, Modal Assurance Criterion, Procedia Engineering, **48** (2012) 543–548.

[19] H. Sohn and C. R. Farrar, Damage diagnosis using time series analysis of vibration signals, Smart Materials and Structures, **10** (2001) 446–451.

[20] J. K. Vandiver, A. B. Dunwoody, R. B. Campbell and M. F. Cook, A mathematical basis for the random decrement vibration signature analysis technique, Journal of Mechanical Design, **104 (2)** (1982) 307–313.

[21] R. Vasheghani Farahani and D. Penumadu, Damage identification of a full-scale five-girder bridge using time-series analysis of vibration data, Engineering Structures, **115** (2016) 129–139.

[22] K. Worden, G. Manson and N. R. J. Fieller, Damage detection using outlier analysis, Journal of Sound and Vibration, **229 (3)** (2000) 647–667.

[23] L. Xie and A. Mita, An innovative substructure damage identification approach for shear structures based on ARMAX models, Procedia Engineering, **188** (2017) 119–124.

[24] Z. Xing and A. Mita, A substructure approach to local damage detection of shear structure, Structural Control and Health Monitoring, **19** (2012) 309–318.